Life Cycle Analysis of Hydrogen Production from Non-Fossil Sources

by

Q. Dai, A. Elgowainy, J. Kelly, J. Han, and M. Wang

Systems Assessment Group

Energy Systems Division

Argonne National Laboratory

September 2016

CONTENTS

FIGURES

TABLES

ACRONYMS

AcOH	acetic acid
BDL	bio-derived liquid
CSL	corn steep liquor
DAP	diammonium phosphate
DOE	U.S. Department of Energy
DOT	U.S. Department of Transportation
EIA	U.S. Energy Information Administration
EPA	U.S. Environmental Protection Agency
FCEV	fuel cell electric vehicle
FCTO	Fuel Cell Technologies Office
GHG	greenhouse gas
H2A	hydrogen analysis
HHV	higher heating value
HTE	high temperature electrolysis
HTGR	high temperature gas-cooled reactor
HTSE	high temperature steam electrolysis
INL	Idaho National Laboratory
LCA	life-cycle analysis
LCI	life-cycle inventory
LHV	lower heating value
MEC	microbial electrolysis cell
NG	natural gas
NGCC	natural gas combined cycle
NRC	National Research Council
NREL	National Renewable Energy Laboratory
PNNL	Pacific Northwest National Laboratory
PSA	pressure swing adsorption
R&D	research and development

SMR	steam methane reforming
SOEC	solid oxide electrolysis cell
TEA	techno-economic analysis
WTW	well-to-wheels
WWTP	wastewater treatment plant

This page intentionally left blank.

Life Cycle Analysis of Hydrogen Production from Non-Fossil Sources

Qiang Dai, Amgad Elgowainy, Jarod C. Kelly, Jeongwoo, Han, and Michael Wang

Energy Systems Division
Argonne National Laboratory

September 2016

1. INTRODUCTION

As a zero-carbon energy carrier, hydrogen is a key component of the advanced fuels and technologies roadmap that the U.S. Department of Energy (DOE) identifies towards a sustainable and clean energy economy (FCTO 2012). U.S. domestic production of hydrogen was around 9 million metric tons per year between 2009 and 2011, and is expected to grow to 11 million metric tons in 2016 (DOE 2012). As of 2016, domestic consumption of hydrogen is primarily for petroleum refining and fertilizer production, while other uses include metal treatment and food processing (EIA 2016a). Although the consumption of hydrogen by the transportation sector is currently very small, EIA has projected a compound annual growth rate of 22.9% in transportation-related hydrogen use between 2015 and 2040, and expects hydrogen consumption for transportation to reach 0.06 quad in 2040, which is equivalent to 0.5 million metric tons based on the lower heating value (LHV) of hydrogen (EIA 2016b). The EIA projection represents the business-as-usual (BAU) case. A more optimistic projection was made by the National Research Council (NRC 2013). With midrange (ambitious but reasonable) technology, low-carbon hydrogen production, fuel cell vehicle subsidies, and other incentives promoting fuel cell electric vehicles (FCEV), it was projected that the annual sales of FCEVs would increase from around 6 million in 2030 to over 12 million in 2040, and remain over 12 million through 2050 (NRC 2013). Assuming that 2050 average age for U.S. light-duty vehicles will remain at current level of 11.4 years (DOT 2016), the NRC projection indicates that over 150 million FCEVs will be on road by 2050. The associated hydrogen consumption by this projected 2050 FCEV fleet will be over 30 million metric tons per year, assuming 12,000 miles traveled annually per vehicle, and an average fuel economy of 60 miles per kg of hydrogen (60 miles per gasoline gallon equivalent) for FCEVs.

Hydrogen can be produced via a wide range of pathways from various sources, among which steam methane reforming (SMR) of natural gas accounts for ~95% of the hydrogen used in the U.S. (DOE 2014). Nevertheless, sustainable hydrogen production from non-fossil sources is a main target of the research and development (R&D) efforts by U.S. DOE and the hydrogen industry (FCTO 2015).

This report conducts life-cycle analysis (LCA) on three non-SMR hydrogen production pathways: dark fermentation of lignocellulosic biomass, high-temperature steam electrolysis

(HTSE) with a solid oxide electrolysis cell (SOEC), and reforming of bio-derived liquids (BDL). The system boundary of this study is well-to-wheels (WTW), which starts with the recovery of the primary feedstock and the production of hydrogen, followed by the delivery of compressed hydrogen to the tank of FCEV, and ends with consumption of hydrogen by FCEV to power its wheels. Material and energy flows along the supply chains of the three hydrogen production pathways are derived from open literature, national laboratory and government agency reports, and engineering calculations. The life-cycle inventory (LCI) tables compiled are to be incorporated into the fuel cycle model of Argonne National Laboratory's Greenhouse gases, Regulated Emissions, and Energy use in Transportation (GREET®) Model for its 2016 release.

2. DARK FERMENTATION OF LIGNOCELLULOSIC BIOMASS

Biological hydrogen production pathways, including photolysis, photosynthesis, dark fermentation, and microbial electrolysis cell (MEC), are categorized as early-development technologies in fuel cell technologies office (FCTO)'s Multi-Year Research, Development, and Demonstration Plan (FCTO 2015). Both photolysis and photosynthesis pathways are driven by sunlight, producing hydrogen from water and organic matter respectively, by specialized microorganisms such as certain strains of algae. In contrast, dark fermentation of biomass generates hydrogen in the absence of light with the help of fermentative bacteria, whereas MEC produces hydrogen from electrolysis of organic matter driven by microbial metabolism and a small amount of external energy. Since the effluent from the dark fermentation process is rich in organic matter, which can be used by MEC to produce additional hydrogen, an integrated pathway combining dark fermentation and MEC has been under investigation by researchers from National Renewable Energy Laboratory (NREL) and Pennsylvania State University (Maness 2015, Maness 2014, Maness 2013, and Maness 2012). This analysis focuses on dark fermentation, MEC, and the integrated pathways. Photolysis and photosynthesis pathways may be examined for future GREET updates.

2.1 Process description

The overall process of hydrogen production from lignocellulosic biomass via dark fermentation combined with MEC is depicted in Figure 1. Corn stover is chosen to be the lignocellulosic feedstock due to data availability. The upstream processes of corn farming and corn stover harvesting already exist in GREET and are used "as is" in this analysis. Note that the upstream greenhouse gas emissions of corn stover harvesting in GREET accounts for the energy use for corn stover collection and transportation as well as the N_2O emissions associated with supplemental N fertilizer use to compensate for nutrients lost with stover removal.

Information about all of processes shown in Figure 1 is obtained from a series of process design and economics reports on biomass conversion published by NREL (Davis 2015, Davis 2013, and Humbird 2011), except for fermentation and MEC. The information for fermentation is based on reports from the NREL group who lead the fermentative hydrogen production research (Maness 2015, Maness 2014, Maness 2013, and Maness 2012), supplemented by Humbird 2011, whereas the information for MEC is obtained from publications by the research group at Pennsylvania State University who developed this process (Lalaurette 2009, Call 2008, Logan 2008, and Cheng 2007). The processes examined in this study start with corn stover handling. Harvested corn stover is milled, and then delivered to the feed handling facilities (Davis 2015). Material and energy requirements for the feed handling process are assumed to be minimal. The biomass is subsequently sent to the biorefinery, in this case a fermentation plant, by truck or rail.

In the fermentation plant, the received biomass enters the pretreatment reactor first. The purpose of the pretreatment process is to break down the matrix of polymeric compounds including cellulose, hemicellulose, and lignin, which constitute the backbone of the cell walls of the biomass. The process is carried out in the sequence of deacetylation with dilute sodium hydroxide at around 80°C, followed by acid pretreatment with dilute sulfuric acid at a higher

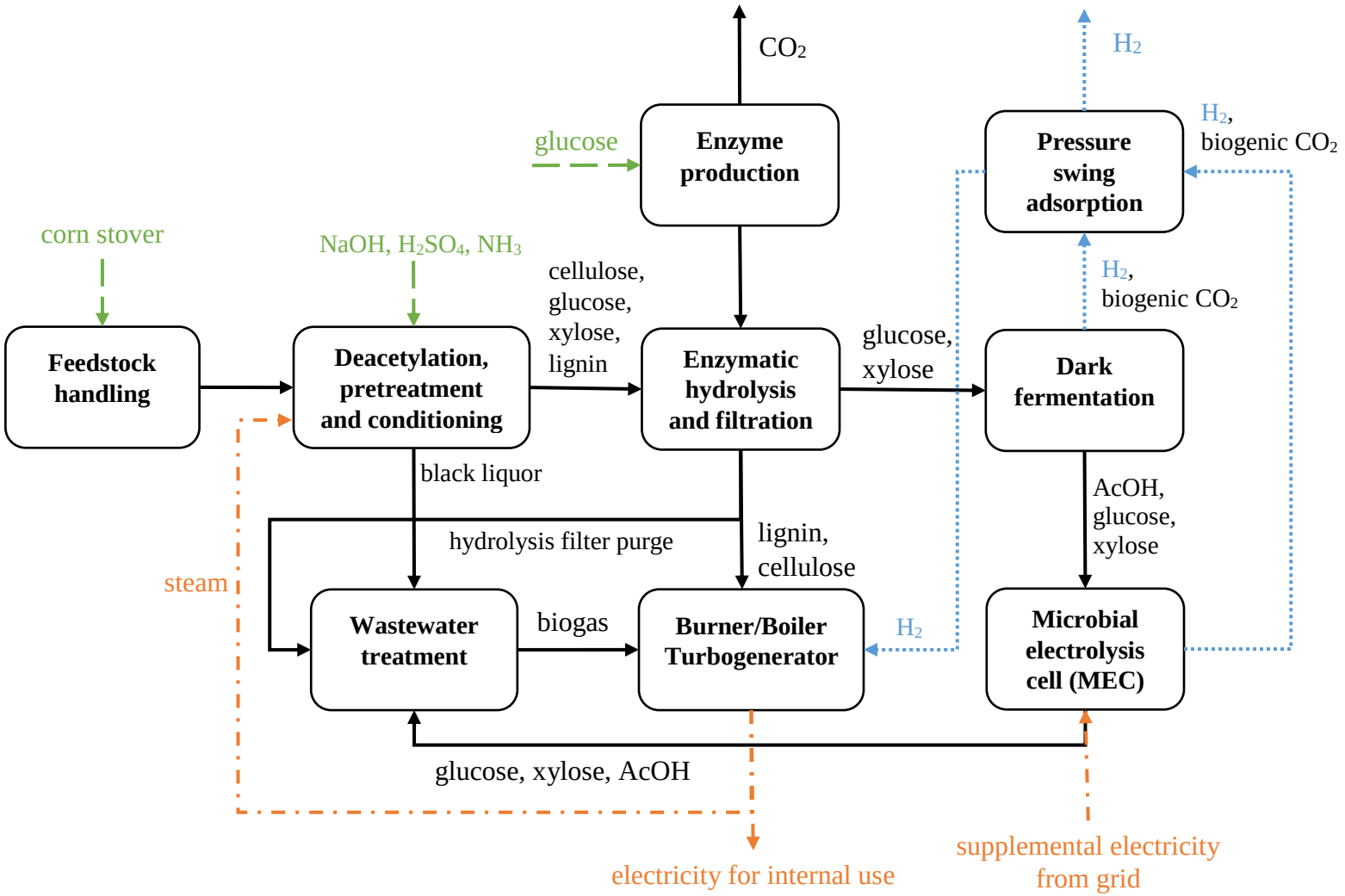

FIGURE 1 Process flow diagram of hydrogen production via fermentation and MEC from corn stover. Green long dash lines represent input material flows; Black solid lines represent intermediate material flows; Blue short dash lines represent hydrogen flows; Orange dotted dash lines represent energy flows.

temperature around 160°C. Heat required by these two steps is provided by steam, which is either produced by a boiler fueled by natural gas, or produced with heat from on-site energy recovery. The pretreated slurry generally contains cellulose, xylose, the majority of lignin, and other insolubles. The drained liquor from the pretreatment process, typically referred to as the "black liquor", is composed of soluble extractives and ash constituents of the biomass, the rest of lignin, and most of the acetate that originally existed in the biomass. The pretreated slurry is then conditioned, during which the pH of the slurry is adjusted to approximately 5 with ammonia, and subsequently sent to enzymatic hydrolysis, whereas the black liquor is sent to a wastewater treatment plant (WWTP) on-site (Davis 2015).

Enzymatic hydrolysis entails the use of enzyme, which is assumed to be produced on-site. The primary carbon source for enzyme production is purchased glucose, which is converted to sophorose as the food source for the enzyme-producing fungus grown aerobically in fed-batch bioreactors. Small amounts of corn steep liquor (CSL) and diammonium phosphate (DAP) are also added in this step as nutrients for the microorganism growth. The broth coming out of the batch reactors is rich in cellulase, and is fed to enzymatic hydrolysis (Davis 2015).

The purpose of enzymatic hydrolysis is the saccharification of cellulose and preferably also xylose. The hydrolysis is initiated in a continuous flow reactor, and is completed in a batch reactor. The slurry coming out of the batch reactor is fed to a vacuum filter press, to remove lignin and other insolubles. The solids fraction of the stream exiting the filter press is sent to a burner for energy recovery. The filtered hydrolysate is concentrated in an evaporator, passed through another filter, and treated by ion exchange, to remove any residues and ions which may deactivate the catalysts used for fermentation (Davis 2015).

The resultant hydrolysate is then sent to the fermenter, where it is cooled, and then inoculated with *Clostridium*, the fermentative bacteria for hydrogen production. In the fermenter, most of the cellulose and xylose are converted to acetic acid (AcOH), ethanol, and lactic acid (see reactions 1, 2, 3 below). Hydrogen is also produced from the fermentation reaction that produces AcOH, and is sent to the PSA unit to be cleaned. The effluent of the fermenter is sent to the MEC for additional hydrogen production (Maness 2015). For the stand-alone fermentation designs, the fermenter effluent is sent to the WWTP.

$$C_6H_{12}O_6 + 2H_2O \rightarrow 2CH_3COOH + 2CO_2 + 4H_2 \quad (1)$$
$$C_6H_{12}O_6 \rightarrow 2CH_3CH_2OH + 2CO_2 \quad (2)$$
$$C_6H_{12}O_6 \rightarrow 2CH_3CHOHCOOH \quad (3)$$

The cell configuration of a MEC is similar to that of a proton exchange membrane fuel cell, as shown in Figure 2. The cathode is a stainless-steel mesh covered by catalysts made of platinum and carbon black, and the anode is a graphite brush. Microorganisms grow on the anode, and hydrogen evolves at the cathode. In the MEC, organic fermentation products, including AcOH, ethanol, and lactic acid, are converted into hydrogen through electrolysis (see reactions 4, 5, 6 below). Electricity input is required to drive the reactions. However, since the electrolysis reactions are facilitated by the metabolism of the microorganisms growing in the cell, less energy is consumed compared with conventional electrolysis of the same organic matter

(Logan 2008). Hydrogen produced from the MEC is sent to the PSA unit for cleaning, while the effluent is sent to the WWTP.

$$CH_3COOH + 2H_2O \rightarrow 2CO_2 + 4H_2 \quad (4)$$
$$CH_3CH_2OH + 3H_2O \rightarrow 2CO_2 + 6H_2 \quad (5)$$
$$CH_3CHOHCOOH + 3H_2O \rightarrow 3CO_2 + 6H_2 \quad (6)$$

Gases collected from the fermenter and the MEC are a mixture of hydrogen, CO_2, a smaller amount of CH_4, and some other trace impurities (Maness 2015, Lalaurette 2009). As a result, the mixture needs to be cleaned to produce hydrogen of higher purity. Since pressure swing adsorption (PSA) is a well-established technology and is widely deployed in SMR facilities, it is selected as the gas cleaning technology for this pathway. It is assumed that PSA operates at 20 bar and recovers 80 wt% of the hydrogen. The unrecovered hydrogen is purged and sent to the combustor for energy recovery.

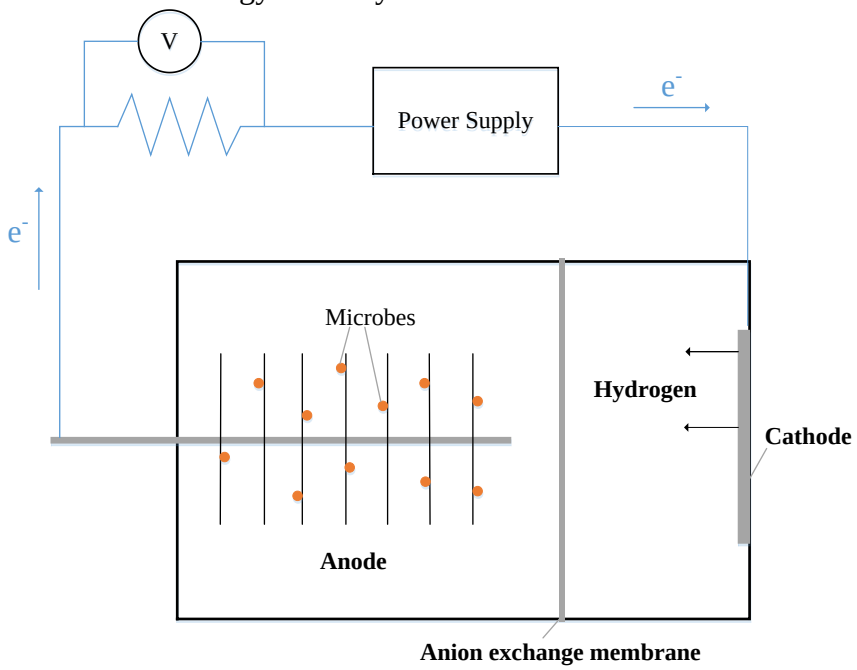

FIGURE 2 Schematic of a MEC (Adapted from Maness 2015)

Wastewater streams are treated in the WWTP by anaerobic and aerobic digestion. Biogas produced from anaerobic digestion is sent to the burner to partially satisfy internal energy demand. The treated water can be recycled and returned to the process (Davis 2015).

The solids from the filter press and WWTP, along with the biogas from the WWTP and the purged hydrogen from the PSA unit, are combusted in the burner to generate steam for heat and power production. The boiler producing the steam is assumed to have an energy efficiency of 80%. The produced steam has a pressure of 62 bar, and a temperature of 454 °C. The steam is sent to a two-stage turbine with an assumed isentropic efficiency of 85%. In the first stage, the steam is expanded to a pressure of 13 bar and a temperature of 268 °C, and a portion of the

expanded steam is diverted to the pretreatment unit to satisfy process heat demand. In the second stage, the steam is fully expanded to a pressure of 0.1 bar. Power is produced from both of the two steam expansion stages, and is used to satisfy part of the on-site electricity demand. Excess electricity is assumed to be exported to the grid (Humbird 2011).

2.2 Material and energy flows

The material and energy flows associated with dark fermentation of corn stover have been reported in DOE's Hydrogen Analysis (H2A) Model (DOE 2016a), as well as a techno-economic analysis (TEA) conducted by NREL (James 2009). The production system in the H2A model is based on a generic fermentation plant, with a capacity of 50,000kg H_2/day, and a capacity factor of 90%. Two scenarios are considered in that model. The first scenario represents "current" hydrogen production without energy recovery, with an overall energy efficiency of only 4.6%. The second scenario represents "future" hydrogen production with energy recovery, with an overall energy efficiency of 65.6%. For energy recovery, it is assumed that lignin is combusted for process heat, whereas filtration effluent containing ethanol, acetate, lactate and formate is sent to wastewater treatment to produce biogas, which is combusted to generate electricity. In addition, the H2A model assumes 90% hydrolysis efficiency for hemicellulose, 98% hydrolysis efficiency for cellulose, a current hydrogen yield of 1.16 moles H_2/mole sugar for both glucose and xylose based on the most recent (as of 2015) lab-data for corn stover fermentation, and a future hydrogen yield of 3.2 moles H_2/mole sugar (DOE 2016a).

TABLE 1 Material and energy flows for corn stover fermentation from the H2A model

	Current	Future
Material inputs		
Corn stover (kg/kg H2)	144.1	49.5
Cooling water (gal/kg H2)	15,255	244
Hemicellulose chemical makeup (kg/kg H2)	1.2	1.2
Nutrient mix (kg/kg H2)	0.1	0.1
Energy inputs		
Electricity (kWh/kg H2)	5.5	2.6
Natural gas (mmbtu/kg H2)	0.2	---
Steam (kg/kg H2)	43	14.8
Process emission		
CO2 (kg/kg H2)	244	79.2
Coproduct		
Electricity (kWh/kg H2)	---	116

The NREL TEA assumes 90% hydrolysis efficiency for both cellulose and hemicellulose, 90% yield for fermentation, 100% conversion rate of glucose and xylose into hydrogen and acetate, and a hydrogen yield of 4 moles H_2/mole glucose equivalent. In addition to dark fermentation, the NREL TEA also examines the MEC pathway and the integrated pathway combining dark fermentation and MEC for hydrogen production. For the MEC pathway, the NREL TEA assumed 90% conversion efficiency for MEC, and cited an electricity consumption of 33.3 kWh/kg H_2. The integrated pathway is configured such that the effluent from the fermenter in the stand-alone dark fermentation pathway is fed to the MEC, while maintaining all the assumed system parameters for both of the stand-alone pathways (James 2009).

TABLE 2 Material and energy flows for corn stover fermentation from NREL TEA

	Fermenter alone	MEC alone	Integrated
Material inputs			
Corn stover (kg/kg H_2)	63.3	---	16.0
Acetic acid (kg/kg H_2)	---	8.7	---
Process water (gal/kg H_2)	7.5	105	76.1
Lime (kg/kg H_2)	1.64	---	0.49
DAP (kg/kg H_2)	0.11	---	0.03
Propane (kg/kg H_2)	0.01	---	0.004
Clarifier polymer (kg/kg H_2)	0.02	---	0.01
Sulfuric acid (kg/kg H_2)	2.14	---	0.64
Energy inputs			
Electricity (kWh/kg H_2)	4.1	37.3	27.5
Process emission			
CO2 (kg/kg H_2)	13.6	11.5	12.2

The material and energy flows reported in the H2A model and the NREL TEA are summarized in Table 1 and Table 2. Information from these two sources are selectively used for inclusion in GREET. The stand-alone dark fermentation process as described in the H2A model is not a realistic process for hydrogen production. Without energy recovery, the proposed pathway consumes around 140 kg of corn stover to produce 1 kg H_2, as opposed to the commercially available process that uses only 17 kg of corn stover to produce 1.5 gallons of ethanol, which is equivalent to 1 kg of H_2 based on energy content (Humbird 2011). With energy recover, the yield and the energy efficiency of the pathway are improved. However, the proposed

system produces over three times of electricity in energy content as hydrogen, and therefore is likely to be categorized as a power plant rather than a hydrogen production plant. The NREL TEA does not provide detailed information for each unit process of the three proposed production pathways, nor can material and energy flows pertaining to each process unit be separated from the system-aggregated LCI.

To be consistent with the GREET pathway of ethanol production from corn stover, the process design and economics reports for biochemical conversion of lignocellulosic biomass published by NREL are selected as the source for the information pertaining to processes other than fermentative hydrogen production, MEC and PSA (Davis 2015, Davis 2013, Humbird 2011). The upstream processes, including feed handling, pretreatment, enzymatic hydrolysis, and enzyme production, are generally the same for all the corn stover conversion pathways described in the three reports regardless of the end products, except that the processes from the more recent reports are incrementally improved and optimized compared to previous versions. Therefore, the material and energy flows for feed handling, pretreatment, enzyme production, and hydrolysis are adapted from those provided in the 2015 report, to represent the best available technology.

TABLE 3 Reported fermentation product mix

	James 2009	Lalaurette 2009	James 2015
Acetic acid	100%	37%	50.6%
Ethanol	---	18%	38.6%
Lactic acid	---	37%	3.6%
Others	---	8%	7.2%

The fermentation process is only discussed in the 2011 NREL report (Humbird 2011). However, the fermentation plant in that report is designed to produce ethanol, as opposed to hydrogen. Since different end products involve the use of different microorganisms, which metabolize differently and require different fermentation conditions, the fermentation process in this study is modeled by our engineering calculation, with an inflow stream (the outflow stream from hydrolysis) obtained from the 2015 NREL report (Davis 2015), and performance parameters reported for fermentative hydrogen production (Maness 2015, James 2015). It should be pointed out that although the fermentative bacteria can utilize both glucose and xylose, it is known to preferentially degrade glucose, which means that the presence of glucose will repress the metabolism of xylose by *Clostridium* (Xiao, 2012). To represent the optimal design for hydrogen production, it is assumed that both glucose and xylose are converted into hydrogen. In addition, the fermentation effluent can be a mixture of AcOH, ethanol, and lactic acid, as mentioned previously in section 2.1, and the mass percentages of these three constituents may vary with fermenter designs and operating conditions as shown in Table 3. Research is being conducted to improve hydrogen yield by selectively inhibiting fermentation pathways that do not produce AcOH, through modifications of the genetics of the fermentative bacteria (Maness 2015, Maness 2014, Maness 2013), since the fermentation reaction produces the most hydrogen on a per mole sugar input basis when the end product is AcOH. In this study, it is assumed that the

fermentation product is 100% AcOH (James, 2009), again, to represent the optimal process design.

Starting from the fermentation process, the system examined in this study deviates from those described in the process design and economics reports by NREL. Nonetheless, the burner, boiler and turbogenerator, as well as the WWTP, are assumed to operate under the same condition, only with different inflows and outflows. Therefore, the burner, boiler, turbogenerator, and the WWTP are modeled with the same process parameters (operating pressures, temperatures, turbine efficiency, boiler efficiency, etc.) as the NREL 2015 report. These process parameters and the modeling are detailed in Appendix A. The material and energy flows are determined based on our engineering calculations, also shown in Appendix A.

The MEC is also modeled in a similar way, but with parameters from the literature. It should be noted that various operating conditions for MECs have been reported (Lalaurette 2009, Call 2008, Logan 2008, and Cheng 2007). The applied voltage to the MEC is of particular interest, since it dictates the external energy requirement of the cell. In general, higher applied voltages result in higher hydrogen production rates (Call 2008), but also lead to higher energy losses and therefore lower cell energy efficiencies (Logan 2008). MEC performance metrics for hydrogen production from AcOH, as reported in different literature, are summarized in Table 4. Numbers within parentheses are ranges, while numbers outside the parentheses are averages. In this study, an applied voltage of 0.6V is assumed, and the corresponding electricity consumption is assumed to be 15 kWh/kg H_2. Note that the ratio of energy in produced hydrogen to the energy in the supplied electricity is denoted as "electrical efficiency", and may exceed 100% because it does not account for the energy embodied in the organic substrates.

TABLE 4 Reported MEC Performance Metrics

	Cheng 2007	Call 2008
H2 yield (mol/mol AcOH)	3.65 (2.01-3.95)	N/A
Applied voltage (V)	0.6 (0.2-0.8)	0.6-0.8
Electricity input (kWh/kg H_2)	15.09[a] (5.78-16.21)	15.51[b] - 20.3[c]

a. Converted from 261% electrical efficiency based on HHV of hydrogen
b. Converted from 254% electrical efficiency based on HHV
c. Converted from 194% electrical efficiency based on HHV

Lastly, 80% of the hydrogen produced from the fermentation and the MEC processes is assumed to pass through a PSA unit. The energy consumption of the PSA unit is assumed to be the same as that of the gas cleaning process used in SMR plants, which is estimated to be 0.175 kWh/kg H_2 (INL 2010). Detailed information on the material and energy flows of each process, assumptions made and engineering calculations done for hydrogen production from fermentation of corn stover are documented in Appendix A.

TABLE 5 Compiled LCIs of systems for hydrogen production via fermentation

	Fermentation		Fermentation and MEC		
	w/out ER	w/ER	w/out ER	w/ER	w/H_2 recovery
Material inputs					
Corn stover (kg/kg H_2)	64.5	64.5	23.0	23.0	23.0
Ammonia (kg/kg H_2)	0.285	0.285	0.102	0.102	0.102
NaOH (kg/kg H_2)	1.09	1.09	0.389	0.389	0.389
H_2SO_4 (kg/kg H_2)	0.580	0.580	0.207	0.207	0.207
Glucose (kg/kg H_2)	0.939	0.939	0.335	0.335	0.335
CSL (kg/kg H_2)	0.022	0.022	0.008	0.008	0.008
DAP (kg/kg H_2)	0.042	0.042	0.015	0.015	0.015
Process water (gal/kg H_2)	77.1	77.1	27.5	27.5	27.5
Energy inputs					
Natural gas (MJ/kg H_2)	64.2	---	22.9	---	---
Electricity (kWh/kg H_2)	18.2	---	21.6	6.03	21.6
Non-combustion emission					
CO_2 (kg/kg H_2)	0.925	0.925	0.330	0.330	0.330
Coproducts					
Electricity to grid (kWh/kg H_2)	---	21.3	---	---	---
AcOH (kg/kg H_2)	18.8	18.8	---	---	---

Based on the data we collected, and the LCA model we developed, the LCIs for five process designs: stand-alone fermentation pathways with and without energy recovery (ER), the integrated pathways with and without ER, and the integrated pathway that recover energy by combusting purged H_2 from the PSA unit only, are compiled and summarized in Table 5. The scenario with H_2 recovery is considered because it improves the system energy efficiency (compared with the scenario without ER) at minimal capital cost (compared with the scenario with ER). The energy recovery unit for the system design with H_2 recovery only consists of a combustor and a boiler, as detailed in Appendix A. The integrated pathway with ER, and that with H_2 recovery, are selected to be incorporated into GREET, since they represent more practical designs for hydrogen production from fermentation of corn stover.

It should be pointed out that CO_2 released from the fermentation of glucose and xylose, the electrolysis of AcOH in the MEC, and the combustion of lignin and biogas in the burner, is assumed to be biogenic since their original carbon is from the biomass feedstock, and therefore are excluded from the LCIs. The CO_2 emissions listed in the LCIs solely arise from the enzyme production through metabolism of glucose by the fungus. Since GREET calculates CO_2 emissions from fuel combustion based on fuel consumptions, these non-combustion emissions need to be added to GREET to complete the carbon balance. Also note that for scenarios without ER, how the lignin is handled will affect the system carbon flow. For example, burning the lignin will lead to carbon neutrality, whereas returning the lignin to soil (e.g. landfill) will possibly generate a carbon credit for carbon sequestration, since a portion of the organic carbon in the lignin will remain inert. As this study focuses on hydrogen production, carbon neutrality is assumed for lignin in all scenarios examined.

3. HIGH-TEMPERATURE STEAM ELECTROLYSIS WITH SOEC

Hydrogen production from high temperature electrolysis (HTE) using SOEC is also a technology having good potential of improving electrolysis efficiency compared to low-temperature electrolysis (FCTO 2015). Electrolysis at higher temperature allows a greater portion of the energy requirement to be provided in the form of heat rather than electricity, as shown in reactions 7 and 8 and Table 6, and also enhances the overall system energy efficiency compared to low-temperature electrolysis (Ni 2008). An integrated system of HTE using SOEC, combined with a high temperature gas-cooled reactor (HTGR) for heat input, is being developed at Idaho National Laboratory (INL), (O'Brien 2014, O'Brien 2012, Harvego 2012).

For water electrolysis, at 25°C,

$$H_2O(vapor) + \frac{228.6kJ}{mol}(electricity) + \frac{13.2kJ}{mol}(heat) \rightarrow H_2 + 1/2O_2 \quad (7)$$

At 1000°C,

$$H_2O(steam) + \frac{179.9kJ}{mol}(electricity) + \frac{69.3kJ}{mol}(heat) \rightarrow H_2 + 1/2O_2 \quad (8)$$

TABLE 6 Energy consumption of hydrogen production via water electrolysis

	Theoretical energy demand at 25°C[a]	Theoretical energy demand at 1000°C[a]	DOE 2020 target for central electrolysis[b]
Electricity (kWh/kg H_2)	31.5	24.8	44.7
Heat (kWh/kg H_2)	1.8	9.5	---

a. Ni 2008
b. FCTO 2015

3.1 Process descriptions

The integrated pathway of hydrogen production with SOEC and HTGR is depicted in Figure 3. A portion of the heat output of the HTGR is diverted to heat up the steam entering the SOEC to around 800°C, and the remaining heat output of the reactor is used for power generation in a gas turbine. Electricity generated from the gas turbine is then sent to the SOEC to drive the HTE. Since hydrogen and oxygen evolve at different electrodes in the SOEC, gas cleaning is not needed for this hydrogen production pathway.

The SOEC is chosen for HTE because it is designed to withstand the high temperature required. A typical SOEC is shown in Figure 4. It contains a cathode made of nickel cermet, an anode made of lanthanum strontium manganite, and an yttria-stabilized zirconia electrolyte. The cell is subject to degradation. The tests conducted by INL showed that the cell lasted about 19 months before efficiency decreased to 80% of initial efficiency (O'Brien 2012).

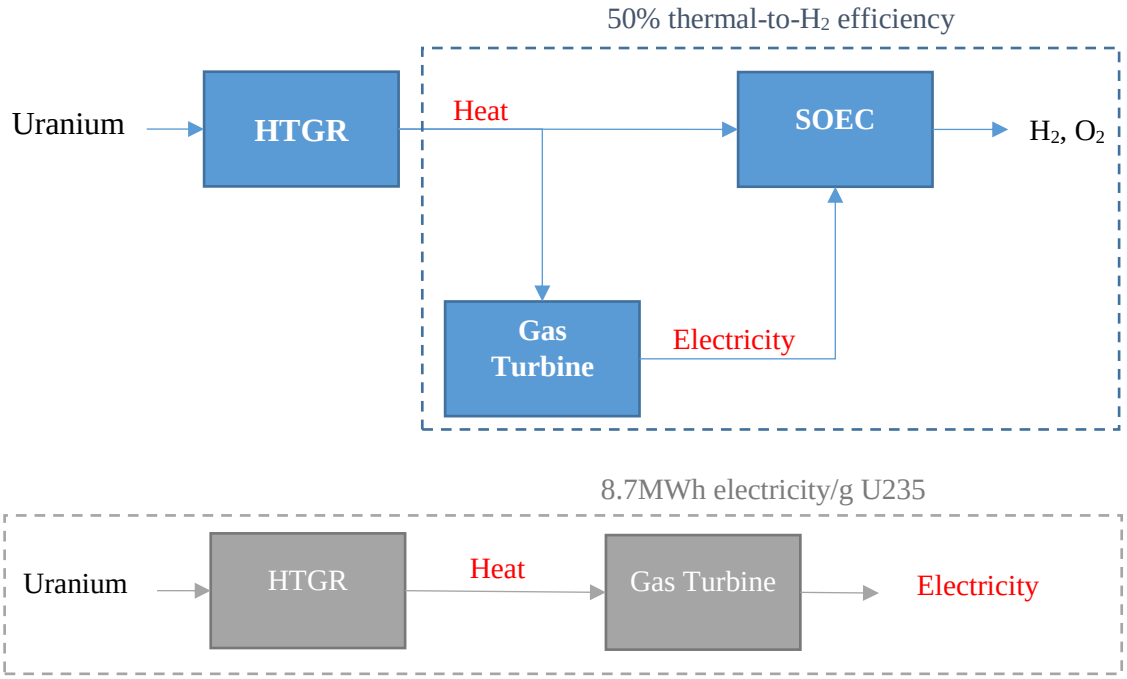

FIGURE 3 Process schematics of hydrogen production via HTE with SOEC and electricity generation with HTGR

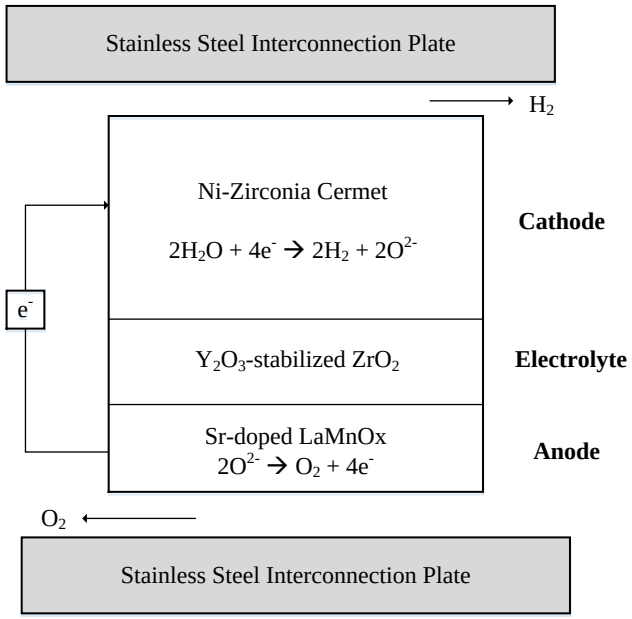

FIGURE 4 Schematic of SOEC (Adapted from O'Brien 2012)

3.2 Material and energy flows

The material and energy flows associated with hydrogen production from HTE have also been reported in the H2A model (DOE 2016a). The production system in the H2A model is based on a conceptual central production plant, with a capacity of 50,000 kg H_2/day, and a capacity factor of 90%. The LCIs compiled from the H2A model are shown in Table 7. However, it is assumed in the H2A model that the production plant utilizes grid electricity for the SOEC, and natural gas-fired heaters to provide the process heat. In other words, it does not represent the integrated HTGR-HTE hydrogen production pathway. As for the process water consumption reported, it seems to be the theoretical water requirement for water electrolysis. Therefore, the H2A LCI is not used in GREET, but serves as the basis of comparison for the natural gas-fueled HTE pathway described later in this section. The material and energy flows of the integrated hydrogen production pathway, are then estimated based on reported system performance metrics and our engineering calculations detailed below.

TABLE 7 Material and energy flows for hydrogen production with SOEC from the H2A model

	Current	Future
Material inputs		
Process water (gal/kg H_2)	2.378	2.378
Energy inputs		
Electricity (kWh/kg H_2)	36.8	35.1
Natural gas (mmbtu/kg H_2)	0.048	0.039
Coproduct		
Oxygen (kg/kg H_2)	7.76	7.77

The thermal efficiency of high temperature helium Brayton cycle at 800-900°C is reported to be 42-46% for 1 turbine-1 compressor configuration, and 53-57% for 3 turbines-6 compressors configuration (Wright, 2006). For the integrated HTE hydrogen production system, it is estimated that about 85% of the thermal energy output of the nuclear reactor is used to drive a Brayton power cycle, which provides the electricity required for the HTE process. The rest of the reactor's thermal output is used to generate steam at around 800°C. The integrated system can achieve an overall thermal-to-hydrogen conversion efficiency of 50% or higher (O'Brien, 2012). A case featuring a hydrogen production rate of 203,558 kg/day from a 600 MWt (MW thermal) nuclear reactor was presented by O'Brien in 2014, which corresponded to a thermal-to-hydrogen conversion efficiency of 47.1% (O'Brien, 2014).

A thermal-to-hydrogen efficiency of 50% is used in this analysis. To produce 1 kg of hydrogen, which has a LHV of 120 MJ/kg, a total thermal heat input 240 MJ/kg H_2 will be

needed. 15% of the heat, which is 36 MJ/kg H_2, is used to produce the steam. The remaining heat of 204 MJ/ kg H_2 is used for power generation in a Brayton cycle. Assuming a 55% efficiency for the high temperature helium Brayton cycle, the produced electricity is calculated to be 31.2 kWh/kg H_2, which seems reasonable compared with the theoretical electricity requirement of 26.2 kWh/kg H_2 for steam electrolysis at 800°C reported in literature (Ni 2008). The HTGR is fueled by uranium. To be consistent with the modeling of HTGR in GREET, the uranium conversion rate of 8.7MWh electricity/g U235 used in GREET is assumed in this study. This rate is converted into 89.5 GJ/g U235 based on the 35% efficiency assumed for the gas turbine in GREET.

For the purpose of comparison, a scenario where natural gas (NG) is used as the energy source for the HTE with SOEC is also considered. In the NG scenario, heat is assumed to be provided by a NG-fueled boiler that is 80% efficient, while electricity is generated from a natural gas combine cycle power plant. The same electricity and heat inputs, 36 MJ/kg H2 and 31.2 kWh/kg H_2 respectively, for the HTGR integrated pathway are assumed for the NG pathway. Accounting for the boiler efficiency, natural gas feed to the boiler is calculated to be 45 MJ/kg H_2. The estimated energy requirements are comparable to those for the future scenario in the H2A model, which consisted of 35.1 kWh/kg H_2 of electricity, and 0.039 mmbtu/kg H_2 (41.1 MJ/kg H_2) of natural gas.

The water requirement for hydrogen production from both of the two HTE pathways is assumed to be the same as that for a central water electrolysis plant (Lampert 2015), the amount of oxygen coproduced is estimated by a stoichiometric calculation. Since the system can produce dry oxygen as a coproduct, allocation based on economic values of produced hydrogen and oxygen is conducted as documented in Appendix B. A hydrogen price of $4.20/kg has been used in GREET, and an oxygen price of $0.20/kg is obtained from Chemicool (Chemicool 2016). The compiled LCI for hydrogen production from HTE in a SOEC with HTGR and NG as the energy sources are summarized in Table 8.

TABLE 8 LCIs for hydrogen production from HTE with SOEC before allocation

	HTGR	NG
Material inputs		
Process water (gal/kg H_2)	2.9	2.9
U235 (g/kg H_2)	0.003	---
Energy inputs		
Electricity from NG (kWh/kg H_2)	---	31.2
Natural gas (MJ/kg H_2)	---	45
Coproduct		
Oxygen (kg/kg H_2)	7.8	7.8

4. STEAM REFORMING OF BDL

Steam reforming of BDL is characterized as a potential distributed production pathway for hydrogen (FCTO 2015). A monolithic reactor for hydrogen production via such pathway is developed at Pacific Northwest National Laboratory (PNNL). The feedstock supplied to the reactor is pyrolysis oil, also known as bio-oil, produced by fast pyrolysis of forest residue (Liu 2015).

4.1 Process description

The process flow diagram of the pyrolysis oil reforming pathway is depicted in Figure 5.

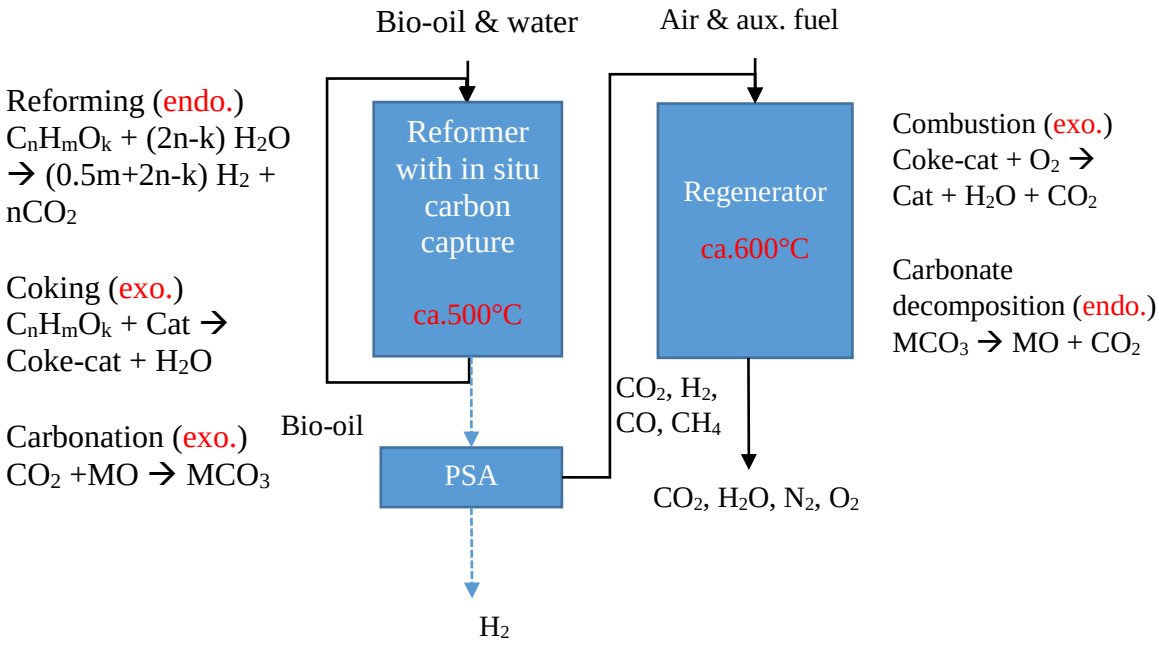

FIGURE 5 Process schematic of hydrogen production from steam reforming of pyrolysis oil. Black solid lines represent material flows; Blue dash lines represent hydrogen flows. Reactions occurring in the reformer are shown on the left; reactions occurring in the regenerator are shown on the right. (Adapted from Liu 2015)

The bio-oil reforming process developed by PNNL features a multi-bed reactor system consisting of parallel reforming and regeneration operations that can be rapidly switched, as a solution to catalyst deactivation and heat transfer challenges. A monolith substrate, which is an array of tiny flow channels separated by a porous wall, is used to build the reactor bed. CO_2 sorbents are filled into alternate channels of the monolith bed, and the steam reforming catalysts are coated onto the open channel walls. The steam reforming catalysts are metal composites typically containing nickel, copper, magnesium, aluminum, and cerium, while the CO_2 sorbents are generally chemical compounds based on magnesium oxide (Liu 2015).

Bio-oil and water enter the reforming reactor, where bio-oil liquid is atomized and sprayed onto the monolith bed. The majority of the bio-oil passing through the reformer is converted into hydrogen via steam reforming. A small amount of the bio-oil feed is converted into coke, which gradually deactivates the catalysts. The unreacted bio-oil exits the reformer, and can be directed back to the reformer inlet to increase the hydrogen yield. The produced gas is a mixture of H_2, CO_2, as well as CO and CH_4 in smaller quantities. Therefore, the gas mixture leaving the reformer is sent to a PSA unit for cleaning. The purged gas from the PSA unit is sent to the regenerator as a supplement needed to satisfy its energy demand. The reforming reactor is designed with in-situ carbon capture for two reasons. Firstly, the CO_2 absorption reaction is exothermic and thus helps to reduce the heat requirement of the reformer. Secondly, since most of the CO_2 is removed from the gaseous output of the reformer, it eliminates the need for a water gas shift after the reformer and also reduces the size of the PSA unit (Liu 2015).

As mentioned earlier, the bed reactor can switch back and forth between reforming mode and regeneration mode. When the CO_2 absorbents become saturated, and the hydrogen yield drops as a result of unfavorable reforming conditions such as low temperature and deactivated catalysts, the reactor is switched from reforming mode to regeneration mode. The purpose of the regeneration operation is to reactivate the catalysts, regenerate the absorbents, and raise the temperature of the reactor back to the optimal temperature for reforming. In the regeneration mode, air is introduced to the reactor to burn off the coke formed on the catalysts. Additional fuel may need to be supplied to the regenerator, if the combustion of formed coke and PSA tail gas cannot completely satisfy the heat requirement of the regenerator. When the regenerator reaches the desired temperature, the metal carbonates decompose to regenerate the CO_2 absorbents. After the catalysts are reactivated, and the CO_2 absorbents are regenerated, the reactor is switched back to reforming mode to continue hydrogen production (Liu 2015).

4.2 Material and energy flows

The BDL pathway has not been incorporated into the H2A model, and no LCI data pertaining to this pathway has been reported in literature. The researchers who had developed this pathway, however, provided key design parameters and major inputs for their bench-scale reactor (Reppe 2016, Liu 2015), which are used to estimate the material and energy flows for the BDL pathway in this analysis as detailed in Appendix C.

Fast pyrolysis of forest residue is modeled in GREET (Han 2011), based on process descriptions and data provided in a PNNL report (Jones 2009). However, the final product of the fast pyrolysis pathway in that report is hydrocarbon liquid fuel (e.g., diesel and gasoline). Although pyrolysis oil was modeled as an intermediate product, the material and energy flows specific to the conversion of forest residue into pyrolysis oil was not available. Rather, pyrolysis oil production and hydrotreating were grouped into one process, and the material and energy inputs for this combined process were reported. In this analysis, it is assumed that fast pyrolysis only needs 30% of the electricity requirement for the combined process, and forest residue is the only material input for fast pyrolysis, since the hydrogen requirement for the combined process would be solely consumed for hydrotreating. Therefore, it is estimated that 0.13 kWh of electricity and 3.19 kg of forest residue are needed to produce 1 kg of pyrolysis oil. Modeling of

the material and energy flows for steam reforming of pyrolysis oil is described in details in Appendix C.

It should be noted that the composition of the pyrolysis oil in GREET is not the same as that of the feedstock for the bench-scale reformer developed by Liu *et al*, as shown in Table 9. The composition of the pyrolysis oil produced from the fast pyrolysis as modeled in GREET is given in an update of the 2009 PNNL report (Jones 2013). Since the composition of the pyrolysis oil dictates the feedstock requirement of the reforming reaction, both compositions are modeled in this analysis. As mentioned earlier, unreacted pyrolysis oil can be redirected into the reformer. Two scenarios, with and without recycling of the unreacted feedstock, are therefore developed for each composition. It should be noted that such pyrolysis oil is unstable due to its high water, oxygen, and olefin content, which leads to phase separation and polymerization if left without a hydrotreating stabilization step for a period of time (~ days). Thus, absent a hydrotreating step, long period of storing pyrolysis oil must be avoided.

TABLE 9 Composition of pyrolysis oil

	Jones 2013	Liu 2015
C	56.6	44.94
H	6.6	7.29
O	36.8	47.66
LHV (MJ/kg)	16.9*	17.4

*This is HHV. LHV is not reported.

The material and energy flows of four process designs for hydrogen production via bio-oil reforming are summarized in Table 10. Again, CO_2 emissions from bio-oil reforming are assumed to be biogenic and are not tracked in this analysis. The process water input and the electricity requirement for equipment and utilities are assumed to be the same for all designs. The BDL reforming development team reported a process water consumption of 5 gal/kg H_2 before PSA, and an auxiliary electricity requirement of 3 kWh/kg H_2 before PSA (Liu 2015). These value are adjusted for 20% hydrogen loss from PSA. As mentioned earlier, the electricity requirement of the PSA is assumed to be 0.175 kWh/kg H_2.

The calculated feedstock requirement for the once-through design based on the bench-scale reformer composition is consistent with the reported value of 11.8 kg bio-oil/kg H_2 after PSA loss adjustments (Liu 2015). Although information on the upstream process of this composition is not available, it is assumed that fast pyrolysis of forest residue occurs at similar conditions regardless of resultant bio-oil compositions. More importantly, since the energy requirement for reforming is much higher compared to the aggregate of the upstream processes, using the reforming process for the reported bio-oil composition is preferable. The designs of reforming with and without recycling based on the bio-oil composition provided by Liu *et al*, are therefore chosen to be incorporated into GREET.

TABLE 10 LCIs for hydrogen production via steam reforming of bio-oil

	Jones 2013		Liu 2015	
	Once-through	Recycled	Once-through	Recycled
Material inputs				
Pyrolysis oil (kg/kg H_2 produced)	9.32	7.45	11.92	9.53
Process water (gal/kg H_2 produced)	6.25	6.25	6.25	6.25
Energy inputs				
Electricity (kWh/kg H_2 produced)	3.925	3.925	3.925	3.925
Natural gas (MJ/kg H_2 produced)	19.3	19.3	---	---

RESULTS, DISCUSSION AND FUTURE WORK

The LCIs for hydrogen production pathways to be incorporated into GREET are summarized in Table 11. Hydrogen transportation by pipeline for a distance of 500 miles from the central plant to the fueling station is added to the fermentation and SOEC pathways, and the universal hydrogen compression process used in GREET to compress the gaseous hydrogen to 900 bar for 700 bar dispensing at the fueling station is added to all the pathways, to complement the WTW LCIs.

TABLE 11 LCIs of hydrogen production pathways for GREET

	Integrated fermentation		HTSE with SOEC		BDL reforming	
	w/H_2 recovery	w/ER	w/HTGR	w/NG	Once-through	Recycled
Material inputs (kg/mmbtu H_2 except for U235 and water)						
Corn stover	202*	202*	---	---	---	---
Pyrolysis oil	---	---	---	---	105	83.8
U235 (g/mmbtu H_2)	---	---	0.021	---	---	---
Ammonia	0.894	0.894	---	---	---	---
NaOH	3.41	3.41	---	---	---	---
H2SO4	1.82	1.82	---	---	---	---
Glucose	2.95	2.95	---	---	---	---
CSL	0.068	0.068	---	---	---	---
DAP	0.131	0.131	---	---	---	---
Water (gal/mmbtu H_2)	242	242	18.6	18.6	54.9	54.9
Energy inputs (mmbtu/mmbtu H_2)						
Electricity	0.181	0.648	---	0.876	0.118	0.118
Natural gas	---	---	---	0.351	---	---
Non-combustion emission (g/mmbtu H_2)						
CO2	2,900	2,900	---	---	---	---

*Converted into 152 dry kg as GREET input, to account for the 25% moisture content (Davis 2015) in the feedstock.

We note that the parameters used for hydrogen production pathways in this analysis are based on laboratory test or bench-scale production. Although performance metrics representing optimal designs for hydrogen production are selected for the modeling in this study, considerable uncertainty exists as to how the pathways would perform when scaled up. For instance, it is estimated that full scale MEC will have an energy consumption of 11.9 kWh/kg H_2 produced (Logan 2008), which is considerably lower than the 15 kWh/kg H_2 assumed in this study, but still significantly higher than the theoretical electricity requirement of 3.45 kWh/kg H_2, thus

providing opportunities for further improvement. The LCIs compiled in this study should be updated with data for optimized mass production once they become available.

Materials used for the production of MEC and SOEC, such as the catalysts used in the BDL pathway, are not included in the LCIs. Since a MEC is similar to a fuel cell, consisting of a graphite anode, a membrane, and a cathode doped with platinum as the catalyst, its environmental footprint could be substantial. Similarly, SOEC contains various rare-earth metals. Given the short life span of a SOEC, its environmental burden may be large when amortized over the hydrogen produced throughout its lifetime. Also, the catalysts for bio-oil reforming may contain nickel, the production of which has environmental concerns. When data becomes available, the contributions of the MEC, the SOEC, and the catalyst for BDL reforming to the WTW environmental impacts of hydrogen should be examined.

Lastly, the process water consumptions reported in this study are preliminary. The water consumption for the fermentation pathway only includes the process water for the pretreatment, hydrolysis, and enzyme production steps due to lack of complete water data, whereas the water consumption for a conventional water electrolysis plant is used as a proxy for the SOEC pathway. These water consumption estimates for these pathways can be improved in future GREET updates.

APPENDIX A MODELING OF THE MATERIAL AND ENERGY FLOWS OF HYDROGEN PRODUCTION FROM DARK FERMENTATION AND MEC

The schematic of the fermentation pathway is shown in Figure 6. Processes are denoted as P1-9, and streams flowing between processes are denoted as S1-10. Table 12 lists all of the stream flows, whereas Table 13 summarizes the material and energy flows for each process. The material balances around the pretreatment unit, hydrolysis unit, fermenter, and MEC, are given in Tables 14-17. Details of the modeling of the WWTP and energy recovery are also provided.

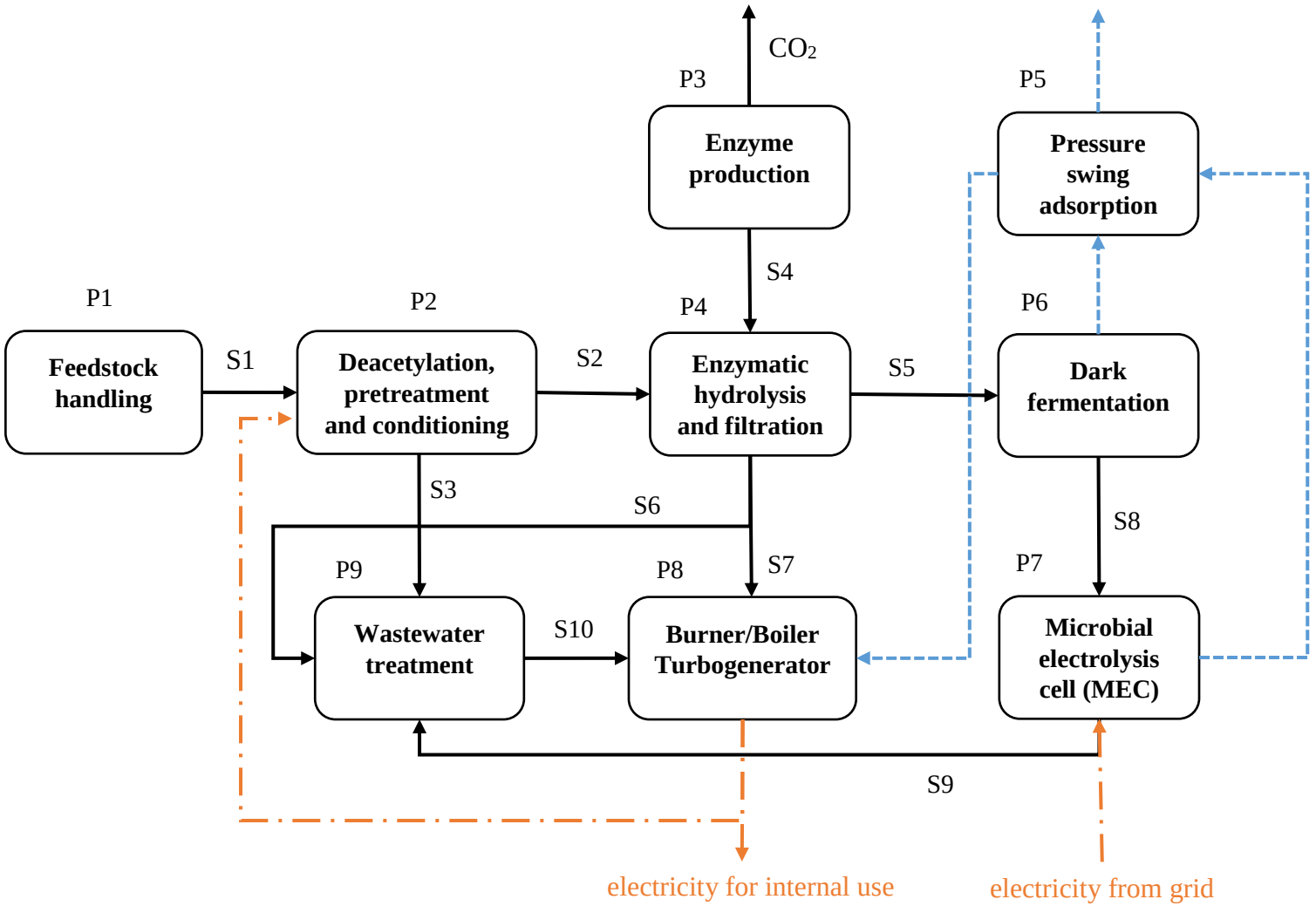

FIGURE 6 Process schematic of hydrogen production via dark fermentation and MEC. Black solid lines represent intermediate material flows; Blue dashed lines represent hydrogen flows; Orange dotted dash lines represent energy flows.

TABLE 12 Stream flows table (kg/hr)

	S1	S2	S3	S4	S5	S6	S7	S8	S9	S10
Water	20,833	258,110	88,642	6,549	304,755	2,819	27,256	294,666	281,581	---
Glucose	---	3,381	---	---	30,838	1,542	311	5,859	5,859	---
Xylose	---	16,310	---	---	16,988	849	172	3,228	3,228	---
Other sugars	642	3,682	321	---	4,181	209	42	3,972	3,972	---
Sugar oligomers	---	559	---	---	1,674	84	17	1,590	1,590	---
Organic solubles	12,208	749	15,421	20	772	28	25	744	744	---
Inorganic solubles	---	1,011	1,406	---	923	---	88	923	923	---
Ammonia	---	---	---	0.1	---	---	---	---	---	---
Sulfuric acid	---	---	---	---	---	---	---	---	---	---
Acetic acid	---	---	7	---	---	---	---	24,232	2,423	---
Furfurals	---	504	332	---	509	10	5	499	499	---
Cellulose	29,205	26,226	---	---	6	3	1,256	3	3	---
Xylan	16,273	415	325	---	2	1	414	1	1	---
Other structural carbonates	3,675	96	---	---	0.5	0.2	95	0.3	0.3	---
Acetate	1,508	---	1,327	---	---	---	---	---	---	---
Lignin	13,132	9,980	2,495	---	50	25	9,955	25	25	---
Protein	2,583	2,583	---	311	15	7	2,887	8	8	---
Other IS	4,108	1,064	---	---	5	3	1,061	2	2	---
Other organics	---	---	---	7	13	7	0.1	6	6	---
Cell mass	---	---	---	54	0.3	0.1	54	0.2	0.2	---
Hydrogen	---	---	---	---	---	---	---	1,615	---	---
CO2	---	---	---	---	---	---	---	17,770	---	---
Biogas	---	---	---	---	---	---	---	---	---	9,577

TABLE 13 Process material and energy flows summary

	P1	P2	P3	P4	P5	P6	P7	P8	P9	Total
Material inputs										
Corn stover (kg/hr)	83,334	---	---	---	---	---	---	---	---	83,334
Ammonia (kg/hr)	---	310	58	---	---	---	---	---	---	368
NaOH (kg/hr)	---	1,406	---	---	---	---	---	---	---	1,406
H_2SO_4 (kg/hr)	---	750	---	---	---	---	---	---	---	750
Glucose (kg/hr)	---	---	1,213	---	---	---	---	---	---	1,213
CSL (kg/hr)	---	---	21	---	---	---	---	---	---	21
DAP (kg/hr)	---	---	54	---	---	---	---	---	---	54
Process water (kg/hr)	---	304,369	5,729	67,177	---	---	---	---	---	377,275
Energy inputs										
Electricity requirement (kW)	859	7,975	1,891	4,834	633	---[a]	54,280	1,502	6,198	78,172
Steam requirement (kg/hr)	---	23,888	---	---	---	---	---	---	---	23,888
Process emission										
CO2 (kg/hr)	---	---	1,195	---	---	---	---	---	---	1,195
Products										
H2 (kg/hr)	---	---	---	---	-905[b]	1,615	2,908	---	---	3,619
Steam (kg/hr)	---	---	---	---	---	---	---	23,888	---	23,888
Electricity (kW)	---	---	---	---	---	---	---	56,360	---	56,360

a. Included in the electricity requirement for P4.
b. Value is negative because hydrogen is diverted to the burner to be combusted.

Pretreatment calculation

It is assumed that during the pretreatment process, 90% of the xylan contained in the feedstock is converted into xylose; 10% of the cellulose converted into glucose; 86% of the lignin is carried into the pretreated slurry and 19% to the black liquor (Davis 2015).

TABLE 14 Mass balance of pretreatment (kg/hr) (Davis 2015)

	Input		Output	
	Feedstock (S1)	Auxiliary	Black liquor (S3)	Pretreated slurry (S2)
Water	20,833	304,369	88,642	258,110
Glucose	---	---	---	3,381
Xylose	---	---	---	16,310
Other sugars	642	---	321	3,682
Sugar oligomers	---	---	---	559
Organic solubles	12,208	---	15,421	749
Inorganic solubles	---	1,406	1,406	1,011
Ammonia	---	310	---	---
Sulfuric acid	---	750	---	---
Acetic acid	---	---	7	---
Furfurals	---	---	332	504
Cellulose	29,205	---	---	26,226
Xylan	16,273	---	325	415
Other structural carbonates	3,675	---	---	96
Acetate	1,508	---	1,327	---
Lignin	13,132	---	2,495	9,980
Protein	2,583	---	---	2,583
Other IS	4,108	---	---	1,064
Total	104,167	330,779	110,276	324,670

Hydrolysis calculation

For the hydrolysis process, it is assumed that 90% of the cellulose in the pretreated slurry is converted into glucose (Davis 2015).

TABLE 15 Mass balance of hydrolysis (kg/hr) (Davis 2015)

	Input			Output		
	Pretreated slurry (S2)	Cellulase (S4)	Auxiliary	Hydrolysate (S5)	Filter purge (S6)	Lignin (S7)
Water	258,110	6,549	67,177	304,755	2,808	27,256
Glucose	3,381	---	---	30,838	1,542	311
Xylose	16,310	---	---	16,988	849	172
Other sugars	3,682	---	---	4,181	209	42
Sugar oligomers	559	---	---	1,674	84	17
Organic solubles	749	20	---	772	28	25
Inorganic solubles	1,011	---	---	923	---	88
Ammonia	---	0.1	---	---	---	---
Sulfuric acid	---	---	---	---	---	---
Acetic acid	---	---	---	---	---	---
Furfurals	504	---	---	509	10	5
Cellulose	26,226	---	---	6	3	1,256
Xylan	415	---	---	2	1	414
Other structural carbonates	96	---	---	0.5	0.2	95
Acetate	---	---	---	---	---	---
Lignin	9,980	---	---	50	25	9,955
Protein	2,583	311	---	15	7	2,887
Other IS	1,064	---	---	5	3	1,061
Other organics	---	7	---	13	7	0.1
Cell mass	---	54	---	0.3	0.1	54
Total	324,670	6,941	67,177	360,732	5,576	43,638

Fermentation calculation

The fermenter is assumed to have a conversion efficiency of 80%, and the fermentation products mix is assumed to be 100% AcOH (James 2015). To simplify the stoichiometric calculation, xylose is modeled as glucose with a pentose to hexose conversion ratio of 0.83. The mass balance of the fermentation process that only converts glucose into hydrogen is also shown for illustrative purposes.

TABLE 16 Mass balance of fermentation (kg/hr)

	Input	Output (fermentation effluent)	
	Hydrolysate (S5)	Converting glucose only	Converting both glucose and xylose (S8)
Water	301,936	297,249	294,666
Glucose	29,296	5,859	5,859
Xylose	16,139	16,139	3,228
Other sugars	3,972	3,972	3,972
Sugar oligomers	1,590	1,590	1,590
Organic solubles	744	744	744
Inorganic solubles	923	923	923
Ammonia	---	---	---
Sulfuric acid	---	---	---
Acetic acid	---	15,625	24,232
Furfurals	499	499	499
Cellulose	3	3	3
Xylan	1	1	1
Other structural carbonates	0.3	0.3	0.3
Acetate	---	---	---
Lignin	25	25	25
Protein	8	8	8
Other IS	2	2	2
Other organics	6	6	6
Cell mass	0.2	0.2	0.2
Hydrogen	---	1,042	1,616
CO2	---	11,458 (biogenic)	17,770 (biogenic)
Ethanol	---	0.0	0.0
Lactic acid	---	0.0	0.0
Total	355,145	355,145	355,145

MEC calculation

In the MEC, it is assumed that 90% of the AcOH is converted into hydrogen (James 2009).

TABLE 17 Mass balance of MEC (kg/hr)

	Input	Output	
	Fermentation effluent (S8)	To WWTP (S9)	To PSA
Water	294,666	281,581	---
Glucose	5,859	5,859	---
Xylose	3,228	3,228	---
Other sugars	3,972	3,972	---
Sugar oligomers	1,590	1,590	---
Organic solubles	744	744	---
Inorganic solubles	923	923	---
Ammonia	---	---	---
Sulfuric acid	---	---	---
Acetic acid	24,232	2,423	---
Furfurals	499	499	---
Cellulose	3.0	3.0	---
Xylan	1.0	1.0	---
Other structural carbonates	0.3	0.3	---
Acetate	---	---	---
Lignin	25	25	---
Protein	8.0	8.0	---
Other IS	2.0	2.0	---
Other organics	6.0	6.0	---
Cell mass	0.2	0.2	---
Hydrogen	---	---	2,908
CO2	---	---	31,986 (biogenic)
Ethanol	0.0	0.0	---
Lactic acid	0.0	0.0	---
Total	335,759	300,865	3,4894

WWTP calculation

For the calculation of biogas released from the WWTP, organic matter is firstly converted to chemical oxygen demand (COD) based on the stoichiometric ratios listed in Table 18, biogas generated in the WWTP from anaerobic metabolism is then estimated by multiplying the aggregate COD by a methane yield rate of 0.23 kg CH_4/kg COD (Ko 2012).

TABLE 18 Substrate to COD ratios

	Sugar	Organics	AcOH	Furfurals	Ethanol	Lactic acid
kg COD/kg substrate	1.07	1.07	1.07	1.67	2.09	1.07

TABLE 19 Mass balance of WWTP (kg/hr)

	Black liquor (S3)	Filter purge(S6)	MEC effluent (S9)	Total	COD
Water	88,642	2,808	281,581	---	---
Glucose	---	1,542	5,859	7,401	7,919
Xylose	---	849	3,228	4,077	4,362
Other sugars	321	209	3,972	4,502	4,817
Sugar oligomers	---	84	1,590	1,674	1,791
Organic solubles	15,421	28	744	16,193	17,327
Inorganic solubles	1,406	---	923	2,329	---
Ammonia	---	---	---	---	---
Sulfuric acid	---	---	---	---	---
Acetic acid	7	---	2,423	2,430	2,600
Furfurals	332	10	499	841	1,405
Cellulose	---	3	3.0	6	---
Xylan	325	1	1.0	327	---
Other structural carbonates	---	0.2	0.3	0.5	---
Acetate	1,327	---	---	1,327	1,420
Lignin	2,495	25	25	2,545	---
Protein	---	7	8.0	15	---
Other IS	0	3	2.0	5	---
Other organics	---	7	6.0	13	---
Cell mass	---	0.1	0.2	0.3	---
Hydrogen	---	---	---	---	---
CO2	---	---	---	---	---
Ethanol	---	---	0.0	0.0	0
Lactic acid	---	---	0.0	0.0	0
Total	110,276	5,576	300,865	43,686	41,641

Burner, boiler and turbocharger calculation

Heat released from combustion of the feed to the burner is calculated by equation 1.

$$\dot{Q}_{burner} = \sum \dot{m}_{feed,i} \times LHV_{feed,i} \quad \text{Eq.1}$$

where $\dot{m}$ represents the mass flow rate of a stream.

LHV values of the feed materials are summarized in Table 20.

TABLE 20 LHV of materials

	Corn stover	Lignin	Cellulose	H_2	Biogas CH_4
LHV (MJ/kg)	17[a]	24[b]	16.5[b]	120	40[c]

a. DOE 2016b
b. Phyllis 2 2016
c. Assumed to be 80% of the LHV of pure methane in GREET to represent biogas

The heat produced from combustion is supplied to a Rankine cycle as depicted in Figure 7 for electricity generation, assuming a boiler efficiency of 80%, and a turbine efficiency of 85% (Davis 2015). Electricity generated by the turbine is calculated by equation 2. Calculations are shown in Table 21 and Table 22.

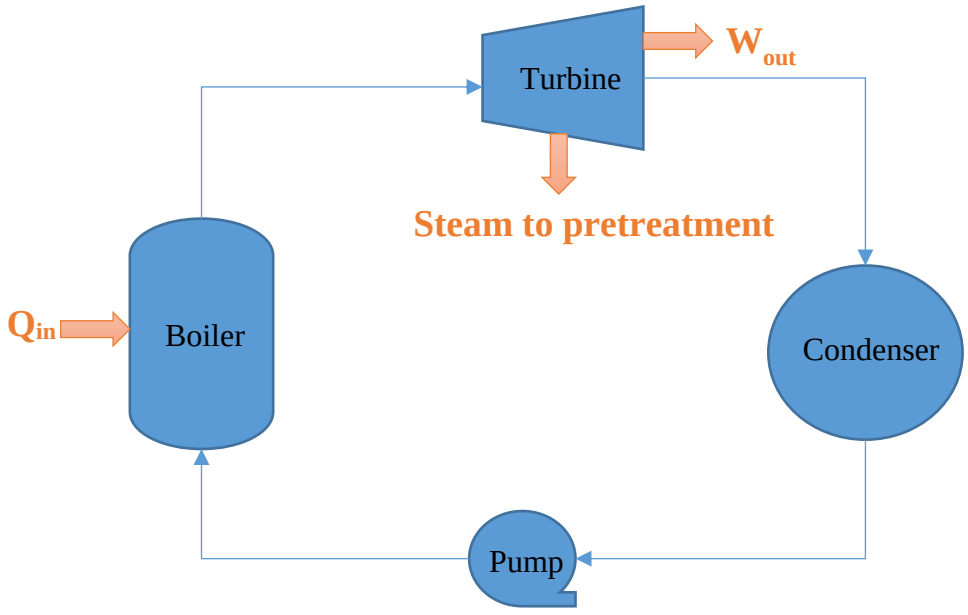

FIGURE 7 Schematic of Rankine cycle electricity generation

$$\dot{W}_{out} = \dot{m} \times (h_{turbine,in} - h_{turbine,out}) \quad \text{Eq.2}$$

where h represents the enthalpy of the steam.

Since the turbine used is not 100% efficient, the enthalpies of the steam coming out of the turbine need to be adjusted for turbine efficiency by equation 3.

$$h_{a,out} = h_{in} - (h_{in} - h_{s,out})/\eta \quad \text{Eq.3}$$

where h_a is the actual/adjusted enthalpy, h_s is the enthalpy found assuming isentropic expansion of the steam, and η represents the efficiency of the turbine.

TABLE 21 Thermodynamic state variables for energy recovery

	P (atm)*	T (°C)*	Steam state	h_a (kJ/kg)	h_s (kJ/kg)	s (kJ/kg.K)
Boiler inlet	62	N/A	saturated liquid	198	N/A	N/A
Boiler outlet/turbine inlet	62	454	superheated steam	3,310	N/A	6.717
turbine outlet 1	13	268	superheated steam	2,976		6.717
turbine outlet 2	0.1	N/A	saturated mixture	2,254	2,127	6.717

*Humbird 2011

TABLE 22 Thermodynamic calculation for energy recovery

	Fermentation		Fermentation and MEC		
	w/out ER	w/ER	w/out ER	w/ER	w/H2 rec
Boiler heat input (MJ/hr)	---	592,774	---	649,023	87,499
Boiler steam output (kg/hr)	---	190,489	---	208,565	28,118
Steam to pretreatment (kg/hr)	---	23,888	---	23,888	23,888
Steam to condenser (kg/hr)	---	166,601	---	184,677	*
Turbine stage 1 work output (MJ/hr)	---	7,979	---	7,979	*
Turbine stage 2 work output (MJ/hr)	---	175,842	---	194,920	*
Total work output (MJ/hr)	---	183,820	---	202,898	*
System heat requirement (MJ/hr)	66,357	66,357	66,357	66,357	66,357
External NG requirement (MJ/hr)	82,947	---	82,947	---	---
System elec. requirement (MJ/hr)	84,547	84,547	281,419	281,419	281,419
External elec. requirement (MJ/hr)	84,547	---	281,419	78,521	281,419
Elec. exported to grid (MJ/hr)	---	99,274	---	---	---
Produced H_2 (kg/hr)	1,292	1,292	3,619	3,619	3,619

*Since not much steam is left after the steam requirement for the pretreatment step is met, it is not sent to the turbine for power generation. In other words, this design only features a burner and a boiler.

For system designs without energy recovery, the steam needed by the pretreatment process is assumed to be produced by a boiler fueled by natural gas, also assuming a boiler efficiency of 80%.

APPENDIX B ALLOCATION BETWEEN HYDROGEN AND OXYGEN FOR HYDROGEN PRODUCTION FROM HTE

Since hydrogen is an energy carrier, while oxygen is not, economic value allocation is not done for the total energy inputs for the two HTE pathways. Rather, only the system energy loss, defined as the difference between total energy input and energy embodied in produced hydrogen, is allocated between hydrogen and oxygen. Allocated energy inputs are calculated by equations 4-6.

$$Allocated\ input_i = Embedded\ input_i + Allocated\ loss_i \quad \text{Eq.4}$$

$$Embedded\ input_i = Energy\ content\ of\ produced\ H_2 \times \frac{Preallocation\ input_i}{\sum Preallocation\ input_i} \quad \text{Eq.5}$$

$$Allocated\ loss_i = (Preallocation\ input_i - Embedded\ input_i) \times Allocation\ ratio_{H2} \quad \text{Eq.6}$$

Where i denotes different types of energy inputs for each hydrogen production pathway.

Based on the unit prices of hydrogen ($4.20/kg) and oxygen ($0.20/kg), and their production volume ratio (7.8 kg oxygen/kg hydrogen), assuming a system producing 1 kg of hydrogen, the economic values of produced hydrogen and oxygen are $4.20 and $1.56, respectively. The allocation ratios are therefore 0.73 for hydrogen, and 0.27 for oxygen.

For the HTE-HTGR pathway, the total energy input is 240 MJ/kg H_2. As the energy content of hydrogen is 120 MJ/kg H_2, the energy loss is 120 MJ/kg H_2. This energy loss is converted into 0.00134g U235/kg H_2, based on the conversion factor of 89.5 GJ/g U235 calculated in section 3.2. 0.001g U235/kg H_2 of the loss is then allocated to hydrogen production. Note that the embedded input is also 0.00134g U235/kg H_2, the allocated input is therefore 0.00234g U235/kg H_2. The allocation for the HTE-NG pathway is shown in Table 23.

TABLE 23 Allocation for hydrogen production from HTE-NG Pathway (MJ/kg H_2)

	Pre-allocation input	Embedded input	Allocated loss	Allocated input
Electricity	112.3	85.7	19.4	105.1
NG	45.0	34.3	7.8	42.1

APPENDIX C MODELING OF THE MATERIAL AND ENERGY FLOWS OF HYDROGEN PRODUCTION FROM BDL

The reforming reaction is given below.

$$C_nH_mO + (2n-1)H_2O \rightarrow nCO_2 + (2n-1+\frac{m}{2})H_2$$

Given the composition of the pyrolysis oil, n and m in its chemical formula can be determined. The stoichiometric coefficients for the reforming reaction can then be derived. Based on stoichiometric calculation, and the assumption that 80% of the pyrolysis oil entering the reformer is converted (64% into hydrogen, and 16% into coke) while the remaining 20% leaves the reformer unreacted (Liu 2015), the feedstock requirement for the production of 1 kg of hydrogen from the system (1.25 kg of hydrogen from the reformer accounting for 20% loss in PSA) can be estimated. The total energy requirement for the process is calculated from the energy content of 1 kg of hydrogen, based on the 80% energy efficiency reported (Liu 2015). The sum of the heat contents of the feedstock and the purged hydrogen from PSA, is then compared with the total energy requirement. If the heat contents are higher than the energy requirement, the system is assumed to be thermally self-sustainable. Otherwise, the energy deficit will be met with auxiliary fuel. The calculation results are summarized in Table 24.

TABLE 24 Calculation of material and energy flows for bio-oil reforming

	Jones 2013		Liu 2015	
	Once-through	Recycled	Once-through	Recycled
n	2.049	2.049	1.256	1.256
m	2.847	2.847	2.428	2.428
% of pyrolysis oil converted into H_2	64%	80%	64%	80%
Feedstock requirement (kg/kg H_2 produced)	9.317	7.454	11.92	9.534
Total energy requirement (MJ/H_2 produced)	150.0	150.0	150.0	150.0
Heat content of converted feedstock (MJ/H_2 produced)	100.8	100.8	132.7	132.7
Heat content of purges H_2 (MJ/kg H_2 produced)	30.0	30.0	30.0	30.0
Total energy input (MJ/kg H_2 produced)	130.8	130.8	162.7	162.7
Self-sufficient?	No	No	Yes	Yes
Auxiliary fuel requirement (MJ/kg H_2 produced)	19.3	19.3		

REFERENCES

Call, D., Logan, B.E., 2008. Hydrogen Production in a Single Chamber Microbial Electrolysis Cell Lacking a Membrane. Environ. Sci. Technol. 42, 3401–3406. doi:10.1021/es8001822

Chemicool 2016. Oxygen. Chemicool Periodic Table. http://www.chemicool.com/elements/oxygen.html (accessed 09/08/2016)

Cheng, S., Logan, B.E., 2007. Sustainable and efficient biohydrogen production via electrohydrogenesis. PNAS 104, 18871–18873. doi:10.1073/pnas.0706379104

Davis, R. *et al*, 2015. Process design and economics for the conversion of lignocellulosic biomass to hydrocarbons: dilute-acid and enzymatic deconstruction of biomass to sugars and catalytic conversion of sugars to hydrocarbons. NREL/TP-5100-62498. http://www.nrel.gov/docs/fy15osti/62498.pdf

Davis, R. *et al*, 2013. Process design and economics for the conversion of lignocellulosic biomass to hydrocarbons: dilute-acid and enzymatic deconstruction of biomass to sugars and biological conversion of sugars to hydrocarbons. NREL/TP-5100-60223. http://www.nrel.gov/docs/fy14osti/60223.pdf

Humbird, D. *et al*, 2011. Process design and economics for biochemical conversion of lignocellulosic biomass to ethanol: dilute-acid pretreatment and enzymatic hydrolysis of corn stover. NREL/TP-5100-47764. http://www.nrel.gov/docs/fy11osti/47764.pdf

DOE 2016a. H2A Production Analysis model version 3.1. https://www.hydrogen.energy.gov/h2a_production.html (accessed 09/12/2016)

DOE 2016b. Biomass Feedstock Composition and Property Database http://www.afdc.energy.gov/biomass/progs/search1.cgi (accessed 09/09/2016)

DOE 2012. DOE Hydrogen and Fuel Cells Program Record #12104: https://www.hydrogen.energy.gov/pdfs/12014_current_us_hydrogen_production.pdf

DOT 2016. Average Age of Automobiles and Trucks in Operation in the United States. http://www.rita.dot.gov/bts/sites/rita.dot.gov.bts/files/publications/national_transportation_statistics/html/table_01_26.html_mfd (accessed 09/27/2016)

EIA 2016 a. Hydrogen Explained: Use of Hydrogen: http://www.eia.gov/energyexplained/index.cfm?page=hydrogen_use (accessed 09/12/2016)

EIA 2016 b. Annual Energy Outlook 2016. http://www.eia.gov/forecasts/aeo/

FCTO 2015. Multi-year Research, Development, and Demonstration Plan: Hydrogen Production: http://energy.gov/sites/prod/files/2015/06/f23/fcto_myrdd_production.pdf

FCTO 2014. Hydrogen Production: http://energy.gov/sites/prod/files/2014/09/f18/fcto_hydrogen_production_fs_0.pdf

FCTO 2012. Multi-year Research, Development, and Demonstration Plan: Introduction: http://energy.gov/sites/prod/files/2014/03/f12/introduction.pdf

Han, J., Elgowainy, A., Palou-Rivera, I., Dunn, J.B., Wang, M.Q., 2011. Well-to-wheels analysis of fast pyrolysis pathways with GREET. ANL/ESD/11-8 https://greet.es.anl.gov/publication-wtw_fast_pyrolysis

Harvego, E.A., O'Brien, J.E., McKellar, M.G., 2012. System evaluations and life-cycle cost analyses for high-temperature electrolysis hydrogen production facilities. INL/EXT-12-25968 https://inldigitallibrary.inl.gov/sti/5436986.pdf

INL, 2010. Sensitivity of hydrogen production via steam methane reforming to high temperature gas-cooled reactor outlet temperature process analysis. INL/TEV-961 https://art.inl.gov/NGNP/INL%20Documents/Year%202010/Sensitivity%20of%20Hydrogen%20Production%20via%20Steam%20Methane%20Reforming%20to%20High%20Temp%20Gas-Cooled%20Reactor%20Outlet%20Temp%20Process%20Analysis.pdf

James, B.D., DeSantis, D.A., Moton, J.M., Houchins, C., 2015. Hydrogen pathways analysis for solid oxide fuel cell (SOFC) and dark fermentation. In *2015 Annual Progress Report* for the DOE Hydrogen and Fuel Cells Program. https://www.hydrogen.energy.gov/pdfs/progress15/ii_a_1_james_2015.pdf

James, B.D. Baum, G.N., Perez. J., Baum, K.N., 2009. Technoeconomic boundary analysis of biological pathways to hydrogen production. NREL/SR-560-46674. https://www1.eere.energy.gov/hydrogenandfuelcells/pdfs/46674.pdf

Jones, S. et al. 2013. Process design and economics for the conversion of lignocellulosic biomass to hydrocarbon fuels: fast pyrolysis and hydrotreating bio-oil pathway. PNNL-23053. http://www.nrel.gov/docs/fy14osti/61178.pdf

Jones, S. et al. 2009. Production of Gasoline and Diesel from Biomass via Fast Pyrolysis, Hydrotreating and Hydrocracking: A Design Case. PNNL-18284. http://www.pnl.gov/main/publications/external/technical_reports/PNNL-18284.pdf

Ko, J.H., Townsend, T.G., Kim, H., 2012. Evaluation of the potential methane yield of industrial wastewaters used in bioreactor landfills. J Mater Cycles Waste Manag 14, 162–168. doi:10.1007/s10163-012-0053-1

Lalaurette, E., Thammannagowda, S., Mohagheghi, A., Maness, P.-C., Logan, B.E., 2009. Hydrogen production from cellulose in a two-stage process combining fermentation and electrohydrogenesis. International Journal of Hydrogen Energy 34, 6201–6210. doi:10.1016/j.ijhydene.2009.05.112

Lampert, D., Cai, H., Wang, Z., Keisman, J., Wu, M., Han, J., Dunn, J., Frank, E., Sullivan, J., Elgowainy, A., Wang, M., 2015. Development of a life cycle inventory of water consumption associated with the production of transportation fuels. ANL/ESD-15/27. https://greet.es.anl.gov/publication-water-lca

Liu, W., Wang, Y., Bertole, C., Xu, B., 2015. Monolithic piston-type reactor for hydrogen production through rapid swing of reforming/combustion reactions. In *2015 Annual Progress Report* for the DOE Hydrogen and Fuel Cells Program. https://www.hydrogen.energy.gov/pdfs/progress15/ii_f_1_liu_2015.pdf

Logan, B.E., Call, D., Cheng, S., Hamelers, H.V.M., Sleutels, T.H.J.A., Jeremiasse, A.W., Rozendal, R.A., 2008. Microbial Electrolysis Cells for High Yield Hydrogen Gas Production from Organic Matter. Environ. Sci. Technol. 42, 8630–8640. doi:10.1021/es801553z

Maness, P.C., Chou, K., and Magnusson, L., 2015. Fermentation and electrohydrogenic approaches to hydrogen production. In *2015 Annual Progress Report* for the DOE Hydrogen and Fuel Cells Program. https://www.hydrogen.energy.gov/pdfs/progress15/ii_e_1_maness_2015.pdf

Maness, P.C., Chou, K., and Magnusson, L., 2014. Fermentation and electrohydrogenic approaches to hydrogen production. In *2014 Annual Progress Report* for the DOE Hydrogen and Fuel Cells Program. https://www.hydrogen.energy.gov/pdfs/progress14/ii_e_3_maness_2014.pdf

Maness, P.C., Chou, K., and Magnusson, L., 2013. Fermentation and electrohydrogenic approaches to hydrogen production. In *2013 Annual Progress Report* for the DOE Hydrogen and Fuel Cells Program. https://www.hydrogen.energy.gov/pdfs/progress13/ii_d_3_maness_2013.pdf

Maness, P.C., Chou, K., and Magnusson, L., 2012. Fermentation and electrohydrogenic approaches to hydrogen production. In *2012 Annual Progress Report* for the DOE Hydrogen and Fuel Cells Program. https://www.hydrogen.energy.gov/pdfs/progress12/ii_g_2_maness_2012.pdf

Ni, M., Leung, M.K.H., Leung, D.Y.C., 2008. Technological development of hydrogen production by solid oxide electrolyzer cell (SOEC). International Journal of Hydrogen Energy 33, 2337–2354. doi:10.1016/j.ijhydene.2008.02.048

NRC, 2013. Transitions to alternative vehicles and fuels. https://www.nap.edu/catalog/18264/transitions-to-alternative-vehicles-and-fuels (accessed 09/27/2016)

O'Brien, J.E., 2014. High temperature electrolysis for efficient hydrogen production from nuclear energy --- INL research program summary. Presentation at Electrolytic Hydrogen Production Workshop. Golden, CO, February 27-28, 2014. http://energy.gov/sites/prod/files/2014/08/f18/fcto_2014_electrolytic_h2_wkshp_obrien1.pdf

O'Brien, J.E. *et al*, 2012. Summary report on solid oxide electrolysis cell testing and development. INL/EXT-11-24261. https://inldigitallibrary.inl.gov/sti/5394148.pdf

Phyllis 2. Database for biomass and waste. https://www.ecn.nl/phyllis2/ (accessed 09/13/2016)

Reppe, K. Personal communication (March 07, 2016)

Wright, S.A., Vermon, M.E., Pickard, P.S., 2006. Concept design for a high temperature helium Brayton cycle with interstage heating and cooling. SAND2006-4147. http://nuclear.inel.gov/deliverables/docs/genivihc_2006_milestone_report_7_1_2006_final.pdf

Xiao, H., Li, Z., Jiang, Y., Yang, Y., Jiang, W., Gu, Y., Yang, S., 2012. Metabolic engineering of d-xylose pathway in Clostridium beijerinckii to optimize solvent production from xylose mother liquid. Metabolic Engineering 14, 569–578. doi:10.1016/j.ymben.2012.05.003